THE DEVELOPMENT AND EVALUATION OF AN EXPERIMENTAL APPARATUS FOR THE INVESTIGATION OF FASTENER PULL-THROUGH FAILURE IN GRAPHITE-EPOXY LAMINATES

Wayne Richard Hanley

NAVAL POSTGRADUATE SCHOOL
Monterey, California

THESIS

THE DEVELOPMENT AND EVALUATION
OF AN EXPERIMENTAL APPARATUS
FOR THE INVESTIGATION OF FASTENER PULL-THROUGH
FAILURE IN GRAPHITE-EPOXY LAMINATES

by

Wayne Richard Hanley

March 1979

Thesis Advisor: R.E. Ball

Approved for public release; distribution unlimited.

REPORT DOCUMENTATION PAGE

READ INSTRUCTIONS BEFORE COMPLETING FORM

1. REPORT NUMBER	2. GOVT ACCESSION NO. / 3. RECIPIENT'S CATALOG NUMBER
4. TITLE (and Subtitle): The Development and Evaluation of an Experimental Apparatus for the Investigation of Fastener Pull-Through Failure in Graphite-Epoxy Laminates	5. TYPE OF REPORT & PERIOD COVERED: Master's Thesis; March 1979
	6. PERFORMING ORG. REPORT NUMBER
7. AUTHOR(s): Wayne Richard Hanley	8. CONTRACT OR GRANT NUMBER(s)
9. PERFORMING ORGANIZATION NAME AND ADDRESS: Naval Postgraduate School, Monterey, California 93940	10. PROGRAM ELEMENT, PROJECT, TASK AREA & WORK UNIT NUMBERS
11. CONTROLLING OFFICE NAME AND ADDRESS: Naval Postgraduate School, Monterey, California 93940	12. REPORT DATE: March 1979
	13. NUMBER OF PAGES: 61
14. MONITORING AGENCY NAME & ADDRESS(if different from Controlling Office)	15. SECURITY CLASS. (of this report): Unclassified
	15a. DECLASSIFICATION/DOWNGRADING SCHEDULE

16. DISTRIBUTION STATEMENT (of this Report)

Approved for public release; distribution unlimited.

17. DISTRIBUTION STATEMENT (of the abstract entered in Block 20, if different from Report)

18. SUPPLEMENTARY NOTES

19. KEY WORDS (Continue on reverse side if necessary and identify by block number)

Fastener Pull-Through Failure
Hyrdraulic Ram
Graphite-Epoxy Laminate

20. ABSTRACT (Continue on reverse side if necessary and identify by block number)

This thesis examines the failure at a fastener hole in a composite fuel tank skin due to hydraulic ram; i.e. fluid pressure due to a penetrating projectile. An experimental apparatus was set up to investigate the triaxial loading conditions at the fastener hole so that an M-P-N failure surface could be developed for the graphite-epoxy laminate. An expression was derived to predict the bending moment at the

(20. ABSTRACT Continued)

fastener in terms of the pull force on the fastener and the axial force in the plate. Aluminum specimens were tested and the results were compared with the predicted results to validate the experimental procedure. The experimental results were found to not be repeatable, and hence a correlation with the predicted results was not appropriate. The non-repeatability could not be explained. Composite specimens were fabricated and prepared for testing. Experimental values for the ultimate pure pull force, P, ultimate pure bending moment, M, and ultimate pure axial force, N, were obtained.

Approved for public release; distribution unlimited.

The Development and Evaluation of an Experimental Apparatus for the Investigation of Fastener Pull-Through Failure in Graphite-Epoxy Laminates

by

Wayne Richard Hanley
Lieutenant Commander, United States Navy
B.S., United States Naval Academy, 1966

Submitted in partial fulfillment of the
requirements for the degree of

MASTER OF SCIENCE IN AERONAUTICAL ENGINEERING

from the

NAVAL POSTGRADUATE SCHOOL
March 1979

ABSTRACT

This thesis examines the failure at a fastener hole in a composite fuel tank skin due to hydraulic ram, i.e. fluid pressure due to a penetrating projectile. An experimental apparatus was set up to investigate the triaxial loading conditions at the fastener hole so that an M-P-N failure surface could be developed for the graphite-epoxy laminate. An expression was derived to predict the bending moment at the fastener in terms of the pull force on the fastener and the axial force in the plate. Aluminum specimens were tested and the results were compared with the predicted results to validate the experimental procedure. The experimental results were found to not be repeatable, and hence a correlation with the predicted results was not appropriate. The non-repeatability could not be explained. Composite specimens were fabricated and prepared for testing. Experimental values for the ultimate pure pull force, P, ultimate pure bending moment, M, and ultimate pure axial force, N, were obtained.

TABLE OF CONTENTS

LIST OF FIGURES

LIST OF TABLES

TABLE OF SYMBOLS

b	Width of plate
C	Distance from neutral axis to stress plane
C1,C2	Constants of integration
D	Flexural rigidity
E	Young's modulus for an isotropic material
F_{cy}	Compressive yield strength
F_{su}	Ultimate shear strength
F_{tu}	Ultimate tensile strength
F_{ty}	Tensile yield strength
h	Plate thickness
I	Moment of inertia
ℓ	Dimension of plate between supports
M	Average moment
M_1	Moment at midpoint of plate
M_o	Moment at origin of plate
M_{ult}	Moment at failure obtained experimentally
M_x	Moment at any point along plate
N	In-plane force
N_{ult}	In-plane force at failure obtained experimentally
P	Pull force in pounds per unit length
P1	Total pull force - input for computer program
P_{ult}	Pull force at failure obtained experimentally
p	Line load per unit length
Q	Shear force

S	Induced tensile load (stretch) per unit length
Sl	Allowable stress
T	Initial axial force in pounds per unit length
U	A parameter equal to $\frac{\ell}{2}\left(\frac{S+T}{D}\right)^{1/2}$
w	Plate deflection
x,y,z	Coordinate axes
λ	Length of arc along the deflection curve
ν	Poisson's ratio
σ_s	Allowable yield stress

ACKNOWLEDGEMENTS

The guidance and assistance provided by Dr. R. E. Ball, the technical support of Mr. R. A. Besel, Mr. T. B. Dunton, Mr. G. A. Middleton and Mr. R. C. Ramaker of the Department of Aeronautics and the contribution by Mr. R. Trabocco of Naval Air Development Center, Warminster, Pennsylvania, have been instrumental in completing this thesis effort and are greatly appreciated.

I. INTRODUCTION

A. ADVANCED COMPOSITES AND THE AEROSPACE INDUSTRY

The most significant technical achievement in the aerospace industry during the next decade will be the application of advanced composite technology to the design and manufacture of primary aircraft and space vehicle structures. Impressive improvements in aircraft weight reduction, performance and cost will be achieved as data is accumulated on advanced composites and additional insight is gained on basic design concepts. Benefits will be derived from both the advanced fiber reinforced composites, which demonstrate excellent specific weight and specific modulus characteristics, and advanced particulate composites where high temperature, high performance structural materials will permit achievement of more efficient thermomechanical power plants. This report is limited in scope to the area of advanced fiber reinforced composites and it reflects the increased interest in composites by the Navy due to the development of the composite wing skin for the F-18.

The decision to pursue the design and development of the F-18 composite wing skin marks the first application of an advanced composite, such as graphite epoxy, as a primary structural component of a production aircraft. This technology advance is not, however, without a certain degree of risk, and the full significance of this step will not be

appreciated until the Hornet has proved itself in the fleet's operational environment.

The use of composites demands that the design engineer evaluate his design in a manner that has not been necessary before. The orthotropic nature of the laminated composite (as opposed to isotropic metals) presents the interesting case where the maximum loading condition may not impose the critical design load. For example, the designer must now consider through-plane shear strength around fasteners in a composite laminate wing skin, whereas the shear strength of metals around fasteners was not critical.

B. INVESTIGATION OF HYDRAULIC RAM EFFECT

A topic which has received considerable attention at the Naval Postgraduate School (NPS), Monterey, California, is the structural integrity of an aircraft fuel tank when it is penetrated by a damage mechanism such as a penetrator or fragment [Refs. 1-6]. This phenomenon is called hydraulic ram. It is the development of shock and pressure waves of destructive intensity in the contained fluid by the passage of a ballistic penetrator through the fuel [Ref. 7]. Pressure waves, resulting from the conversion of the kinetic energy of the projectile to hydraulic pressure, act at the fuel cell boundaries and can cause catastrophic failure of the tank walls, as shown in Fig. 1.

Reference 3 describes hydraulic ram failures of a fuel cell with a composite laminate skin. The intense fluid

pressure on the composite wall caused bending, stretching and shearing forces in the plate at the clamped boundaries. The large bending, in-plane and shearing strains encountered exceeded material limits causing gross failure. For the same loading, boundary conditions and plate dimensions, the composite laminate was found to be significantly weaker than an aluminum plate in through-plane shear.

An investigation into the structural consequences of hydraulic ram requires an understanding of the complex stress conditions in the laminate in the vicinity of the wall boundary. This stress field depends upon the method of attachment to the underlying structure, i.e. ribs, spars, etc. There are two primary means of attachment used in the construction of a composite structure. The first, adhesive bonding, is the joining of two or more components or surfaces by means of a bonding agent in such a manner that the joint is capable of transmitting significant structural loads [Ref. 8]. The load reaction is uniformly distributed along the entire length of the joint. The second is the mechanical fastener, where the reaction is concentrated at each fastener. Figure 2 shows both an adhesive bonded joint and a mechanically fastened joint. Combinations of the two methods of fastening are also used.

C. THE FASTENER PULL-THROUGH PROBLEM

In the F-18 wing design, several factors influenced the choice of attachment method. A critical requirement for the

use of a graphite-epoxy laminate material was the need for access to both surfaces of the skin to monitor its condition. Repairability and replaceability were also requirements [Ref. 9]. For these reasons, mechanical fasteners were specified for attaching the skin to the ribs and spars. Tests involving fastener holes in small test specimens established design allowables in tension and compression at room temperatures, which were used to size the F-18 wing skin for conventional operational loads. Hydraulic ram was not considered. Consequently, several questions should be considered. Will the critical failure mode be failure in tension or compression? To what degree should shear failure be considered? Will there be a problem with fastener pull-through as shown in Fig. 3?

Reference 4 was a first attempt to investigate the fastener pull-through problem. The relationship between the bending moment, M, and the shear force, Q, at the fastener hole of a composite plate due to a pull force, P, on the fastener was determined. Tests were conducted on four inch wide flat aluminum plates and four inch wide composite laminate specimens to determine the pull force required to cause joint failure, i.e. fastener pull-through, for varying specimen lengths. The test set-up is shown in Fig. 4.

The pull force was measured experimentally. The statically determinant test set up provided the bending moment across the specimen directly. Varying the specimen length provided different combinations of M and P at failure. Experimental

values of M and P at failure were non-dimensionalized with respect to the values at failure under pure bending and shearing conditions respectively. Plots of the non-dimensional moment versus the non-dimensional shear at failure were constructed to develop an M-P failure curve for the composite material.

The investigation was incomplete in that in-plane tensile stresses, which will occur due to hydraulic ram, were not considered. The addition of an in-plane force, N, is required for a complete idealization of the problem, leading to a M-P-N failure surface. Using this failure surface, a designer can determine the maximum allowable reaction force, P, at a fastener when the wall is subjected to a specified bending moment, M, and in-plane force, N.

D. THESIS OBJECTIVES AND REPORT ORGANIZATION

This thesis is a continuation of the study of the fastener pull-through failure problem begun in Ref. 4. The objectives of the thesis were: 1) to develop an experimental apparatus that would create an M-P-N loading condition in four inch wide aluminum and composite plate specimens, 2) to construct composite test specimens, and 3) to use the experimental set-up to determine the M-P-N failure surface for the graphite-epoxy laminate studied.

The composite wing structure of the F-18 aircraft was idealized as a four inch wide plate specimen. Composite specimens of the idealized wing structure were prepared.

The experimental apparatus to obtain normal and shear failure stresses was set up. A prediction method was derived to express the bending moment in terms of pull force and axial force parameters. Aluminum specimens were fabricated and tested to validate the experimental procedure in comparison with the prediction method. Testing of composite specimens was begun.

II. PROBLEM DEFINITION

A. IDEALIZATION OF THE WING

The experimental set-up represents the lower wing surface of a wet-wing aircraft, partially filled with fuel, on a high speed, high "g" pull-out from an ordnance delivery mission. The tension loaded wing skin is penetrated by a round of enemy anti-aircraft fire which generates hydraulic ram. The stress environment in the skin consists of the stresses due to pull-out and those due to the ram pressure normal to the wing surface. The fluid pressures produce three types of internal forces in the skin, in-plane tensile forces, N, thickness or through-plane shear forces, Q, and bending moments, M.[1] The reactions to these forces are concentrated at the fastener head causing high stress levels there, as shown in Fig. 2.

B. TEST SPECIMENS

The four inch wide plate specimen with a single fastener hole in the middle, shown in Fig. 5, provides an approximation of the wing surface over a spar and a rib. Spar and rib specimens must be considered separately due to the orthotropic nature of the laminate, as shown in Fig. 6. This feature is described in Ref. 4. The specimens are

---

[1] Twisting of the skin is neglected.

loaded and supported as shown in Fig. 7. Clamped boundary conditions are imposed at the two ends of the specimen, and the two sides are free. In Ref. 4, the ends were simply supported, thus providing a statically determinate specimen. In this study, the clamped ends were necessary in order to introduce the in-plane force, N. This leads to a statically indeterminate structure. The important parameters to be determined are M, N and P at the hole.

The in-plane force, N, consists of an initial in-plane force, T, applied at the boundaries and a stretching force, S, due to the pull force applied at the fastener. As the pull force is applied, it causes a deflection of the specimen. Because of the clamped boundary condition at the ends, which restrains the ends from movement, a tensile force develops in the plate which resists the deflection. This induced axial load, S, is dependent on both the pull force, P, and the initial force, T.

C. COMPOSITE TEST CONSIDERATIONS

An investigation of the triaxial loading condition at the mechanical fastener must consider the orthotropic nature of the composite. Alignment and stress concentration effects are magnified by its high modulus and low strain characteristics. The inherently low inter-laminar shear strength of the composite affects the manner of gripping of the test specimen and the means of load transfer. The specimen aspect ratio, i.e. length to width, is a critical factor in

testing cross-plied laminates. An induced transverse stress results when low aspect ratio, i.e. very wide, specimens are tested. When the diagnoal filaments are continuous from one end to the other, a variable longitudinal stress and an unknown transverse stress result. The general testing procedure should provide a uniform stress over the entire test section of the specimen. The load application must be such that unwanted stresses are eliminated. The test should be representative of the intended application considering size effects, fabrication, rate of loading and environment.

Under almost any test procedure, shear measurements are difficult to obtain. In multiaxial loading experiments, the generation of uniformly stressed test specimens is difficult because of the lack of isotropy, the stiffness and inelastic regions which result in sensitivity to section change, edge restraints and restrictions in allowable stress and Poisson's ratio which may exist [Ref. 10].

The four inch specimen used in this study minimizes the difficulties encountered when testing composites since there are no continuous diagonal filaments running from one end to the other. Furthermore, although a significant stress concentration exists at the fastener hole, its effect on the strength of the specimen is an integral part of the actual pull-through problem.

III. DESCRIPTION OF APPARATUS SPECIMENS AND TEST PROCEDURE

A. TEST APPARATUS

The Aeronautics Department's Reihle Universal Testing Machine was used to impose a range of constant tensile loads, N, on the aluminum and laminated test specimens. It was modified to accept a horizontally mounted hydraulic cylinder with which the transverse or through-plane pull force, P, was applied. Cylinder rod movement was controlled by a manually operated dual chamber hydraulic pump. Affixed to the piston rod was a Baldwin SR-4 Load Cell wired to a wheatstone bridge. Read outs in pounds of pull force were displayed on a digital indicator. The wheatstone bridge was also connected to a strip chart to maintain a time history of the load application. The pull force was applied to the composite specimen by means of a threaded Hi Lok Hi Tigue pin with protruding shear head as in Ref. 4. The digital display was monitored during the conduct of the experiment. Corresponding tensile loads were tabulated for various pull forces at the desired span dimensions, ℓ. Figure 8 is a photograph of the experimental layout.

The value used for the tensile load, N, is the axial load applied by the Reihle Testing Machine. The pull force, P, is taken as the force applied by the hydraulic cylinder. The bending moment, M, is more difficult to assess directly from experimental values. It is a function of the deflection of the plate as well as of the pull and tensile forces, and

thus a relationship between the variables is necessary. Section IV contains a derivation of the expression for M.

B. ALUMINUM SPECIMEN FABRICATION AND TEST PROCEDURE

Aluminum specimens were prepared by the NPS Machine Shop and used to evaluate the experimental procedure as well as to verify the prediction method for calculation of M. Each specimen was cut from 7075-T6 sheet aluminum. A hole was drilled in its center.

A uniform bending moment across the specimen was obtained by using a one-half inch diameter solid steel cylinder centered on a Hi Tigue pin as described in Ref. 4 and shown in Fig. 9.[2] The pin was inserted through the hole in the specimen and attached to the hydraulic cylinder as previously described. Pulling on the fastener pulled the cylinder against the back surface of the plate.

The specimen was then inserted in the grips of the Reihle Testing Machine. Care was taken to ensure that the specimen was oriented vertically. The pin was attached to the hydraulic cylinder by means of a counter-sunk, threaded bar stock rod. The hydraulic cylinder was checked to ensure that the pull force was horizontal and normal to the plate.

Both the testing machine and the load cell/wheatstone bridge arrangement were zeroed. The desired tensile load

---

[2]The moment was not exactly uniform due to the presence of the hole.

was applied and stabilized after the grips had been set. The hydraulic pump was then activated to apply the pull force. The tensile force changed as the pull force was applied. This feature is discussed further in Section V.

Nine 7075-T6 Aluminum specimens were subjected to uniform bending as described above. Experimental results are discussed in Section V.

C. COMPOSITE PLATE LAY UP AND TEST PROCEDURE

Two 16 inch by 16 inch and three 15 inch by 15 inch composite plates were prepared in the Aeronautics Department Composites Lab using the equipment described in Ref. 11. Hercules 3501-6/AS (High Strength) pre-preg tape was used to lay up the composite plates. The plates were cut into four inch wide test specimens of varying lengths. Both 12 inch wide, nominal 10.4 mil thick and three inch wide, nominal 5.2 mil thick tapes were used. Eight ply $[0/\pm45/90]_s$ balanced, anti-symmetric laminates were fabricated from the 10.4 mil tape while the 5.2 mil tape was used to lay up 16 ply $[(0/\pm45/90)_2]_s$ balanced, anti-symmetric laminates. The resultant plates were approximately the same thickness. The cure cycle was a modification of the standard cycle recommended by Hercules in Ref. 12. Pressure was applied using the Wabash Hydraulic Press with electrically controlled heated upper and lower patens. Temperature and pressure control was maintained by a Leeds and Northrop Speedomax-H strip chart recorder modified with a gear-train drive, set

for a constant temperature ramp, and an adjoining Series 60 control unit connected to the press. The cure cycle utilized the ramp from room temperature to 275°F at which temperature the specimen was held for 58.5 minutes. This dwell assured complete and uniform temperature distribution throughout the specimen to facilitate the initial cure process. A pressure of 65 psi was then applied and the composite material was heated to 350°±5°F in 14.9 minutes. A dwell of 120 minutes accomplished the cure. Heat was removed and the composite plate was allowed to cool, still under pressure, to less than 140°F. A post cure was then conducted at 350°F for eight hours in the Blue M Electric Oven as recommended by Ref. 12. Figure 10 is a photograph of the equipment used in the fabrication of the graphite-epoxy laminates. The plates were cut with a water-cooled lapidary saw into four inch wide specimens with lengths varying from 5 1/2 inches to 10 inches. Thirty-three specimens were made up. Five specimens each were made up for use in ultimate shear, ultimate bending and ultimate pull-force testing. Eighteen specimens have been prepared for use in fastener pull-through failure testing. Table I lists the specimen number, orientation and length.

Two inch by four inch copper sheathed fiberglass grips were epoxied to each tensile test specimen to preclude crushing the specimen and to prevent slipping in the test machine. A one-quarter inch diameter hole was drilled in

the center of each specimen witha diamond embedded drill bit using kerosene for cooling and lubrication to minimize distortion at the edges of the hole.

Ultimate shear force and ultimate bending moment were obtained for each composite plate in the same manner as in Ref. 4. Figure 11 is a photograph of the test set up in which a line load, applied by pulling the half inch solid steel cylinder against the composite specimen as described in Section III for aluminum specimens, to obtain an ultimate bending moment value. The ultimate shear force was determined by pulling a Hi Tigue pin through a two inch by two inch composite specimen restrained by a 5/8 inch steel plate with a 35/64 inch diameter hole through which the pin was drawn. Figure 12 is a photograph of the experimental apparatus. Ultimate tensile load was determined for each composite plate by loading the specimen in tension in the testing machine until failure occurred.

IV. ANALYSIS FOR THE BENDING MOMENT

Reference 12 describes the procedure for determining the stresses in a long rectangular plate with a uniform pressure and built-in edges to prevent rotation or deflection. The derivation is based on the following assumptions.

1. Plane cross-sections remain plane.
2. The deflection is a developable surface.
3. The deflection is small with respect to the length of the plate.
4. The plate is elastic and isotropic.

The differential equation for the deflection of the plate is

$$D\left(\frac{d^2w}{dx^2}\right) = -M \qquad (1)$$

where M is the bending moment per unit length at any cross-section of the plate and D is the flexural rigidity

$$D = \frac{E\,h^3}{12(1-\nu^2)} \qquad (2)$$

An expression for the deflection of the plate can be derived in terms of its dimensions, ℓ and h, and u, a parameter which is used to determine S, the induced tensile load per unit length which prevents movement of the ends of the plate. The difference between the arc along the deflection curve and the original chord is determined using the equation

$$\lambda = \frac{1}{2} \int_0^{\ell} \left(\frac{dw}{dx}\right)^2 dx = \frac{S(1-\nu^2)\ell}{hE} \qquad (3)$$

Applying boundary conditions and utilizing symmetry, an expression for the deflection is obtained which when inserted into equation (3) leads to an expression in terms of u. This expression is plotted for various values of u. For a given set of conditions the graph is used to obtain a value of u. The maximum stress can then be determined for this value of u.

The idealized wing skin, which includes an existing tensile force, T, in the x direction, as shown in Fig. 13, can be analyzed in a similar manner. From the figure, the moment is seen to be

$$M = -M_o - \frac{px}{2} + w(S+T) \qquad (4)$$

An expression for the deflection, w, is obtained by substituting equation (4) into equation (1) and introducing the value

$$\frac{S+T}{D} = \frac{4u^2}{\ell^2} \qquad (5)$$

where S equals the force due to elongation and T is the existing tensile load per unit length in the skin.

The solution of this differential equation is of the form

$$w = C_1 \sinh \frac{2ux}{\ell} + C_2 \cosh \frac{2ux}{\ell} + \frac{P\ell^2 x}{8u^2 D} + \frac{M_o \ell^2}{4u^2 D} \qquad (6)$$

Applying the clamped boundary conditions and the condition of symmetry

$$w = 0 \qquad \text{at} \quad x = 0 \qquad (7a)$$

$$\frac{dw}{dx} = 0 \qquad \text{at} \quad x = 0, \frac{\ell}{2} \qquad (7b)$$

to equation (6) leads to the following expressions for the constants of integration, C_1 and C_2, and the bending moment, M_o, at the clamped edge

$$C_1 = \frac{-p\ell^3}{16u^3 D} \qquad (8a)$$

$$C_2 = \frac{p\ell^3}{16u^3 D} \tanh \frac{u}{2} \qquad (8b)$$

$$M_o = \frac{p\ell}{4u} \tanh \frac{u}{2} \qquad (9)$$

After simplifying, the expression for the deflection becomes

$$w = \frac{-p\ell^3}{8u^3 D} \left[\frac{\cosh \left(\frac{u}{2} - \frac{ux}{\ell}\right) \sinh \frac{ux}{\ell}}{\cosh \frac{u}{2}} \right] + \frac{p\ell^2 x}{8u^2 D} \qquad (10)$$

Substituting the slope of the deflection into equation (3), and rearranging terms leads to the expression which is used to determine u for the given parameters.

$$\frac{D^2h^2}{3p^2\ell^6} = \frac{1}{128u^6} - \frac{\tanh \frac{u}{2}}{32u^7} + \frac{\sinh u + u}{128u^7(\cosh u + 1)} + \frac{Th^2D}{12u^2p^2\ell^4} \qquad (11)$$

The deflection at the midspan, $x = \frac{\ell}{2}$, becomes

$$w = \frac{p\ell^3}{16u^2D}\left[1 - \frac{2 \tanh \frac{u}{2}}{u}\right] \qquad (12)$$

and equation (4) can be used to obtain an expression for M at $x = \frac{\ell}{2}$.

$$M_{\ell/2} = \frac{p\ell}{4u} \tanh \frac{u}{2} \qquad (13)$$

The total stress at any cross-section consists of a bending stress and a tensile stress and can be calculated from

$$\sigma_m = \frac{6M}{h^2} + \frac{S + T}{h} \qquad (14)$$

for isotropic plates, note that

$$N = S + T \qquad (15)$$

The solution for u, and hence M, can be obtained by rearranging equation (11) with all terms on the right hand

side and setting it equal to zero. The desired value of u is that value for which the right hand side of the equation is equal to zero. It can be determined using an iterative process. Appendix A is a Basic Language program for the Hewlett Packard 9830 Computer which determines u. The total axial forces developed in the wing skin for a given initial tensile load and desired pull force and the moment at the mid-point are also calculated, as are values for deflection and total stress.

V. RESULTS AND DISCUSSION

A. ALUMINUM SPECIMENS

Aluminum specimens were tested in the experimental apparatus to verify that the test results were repeatable and that there was a correlation with the results predicted by the analysis given in Section IV. Initial tests revealed slipping at the grips. After the tensile load was set, and the pull force effects investigated, the release of the pull force, i.e. returning it to zero, would not restore the initial tensile load. The resultant load after conducting the pull test was significantly less than that first set. This presented a problem because it is necessary to accurately predict the axial tension in order to accurately predict the bending moment. With slippage, the value for T was significantly less than the initial value set on the testing machine. This results in an erroneous value for u and an inaccurate moment calculation.

The effect of slippage was minimized by increasing the axial tensile force to a value greater than the desired initial axial force but still below the yield stress for the material. The force was then reduced to the desired axial load. This process was sometimes repeated more than once to ensure that the grips were properly set and that slippage would not occur.

Two series of tests were conducted to evaluate the accuracy and repeatability of the test procedure. Figures 14 (a-i) are graphs comparing the values of measured axial forces versus the measured pull force and the corresponding predicted results. For ease of comparison, the forces are given in pounds, i.e. in pounds per unit length times the specimen width. Each graph corresponds to a different length specimen and different value of T. The origin for the abscissa indicates the initial axial load applied by the Reihle Testing Machine for zero pull force. The curves represent the total axial load, N, which is the sum of the initial axial load, T, and the load resulting from stretching the aluminum plate.

An alternative means of presenting predicted results for the pull-through problem is shown in Fig. 15. This plot has initial axial load plotted versus total axial load for constant pull force. Several values of pull force are shown on the graph. In this manner a known loading condition of initial axial force and desired pull force will permit determination of the total axial force generated. Using this value and the corresponding moment, the total stress can be calculated and checked against yield stress.

Examination of Figs. 14 (a-i) reveals that, in general, the results for S + T are not repeatable and they are not in good agreement with the predicted values. Note that the results from the second series of tests are closer to the

predicted values than the first series. Also, the results for the shorter specimens appear to be in better agreement with the predicted values than those of the eight inch specimens.

During the experimental procedure, the hydraulic cylinder was checked with a level to ensure that the pull force was applied normal to the specimen surface and that it was oriented in a direct line with the fastener head. The vertical orientation was verified when it was placed in the testing machine.

Manual activation of the hydraulic pump supplied pressure to the pull-force cylinder in a non-uniform manner. Between strokes and, on occasion, while pumping, an apparent reaction or lack of response to the increasing pull force was noted. Uniform application of the pull force may achieve some improvement in experimental results.

The non-repeatability of the test results for the aluminum specimens raises serious questions about the validity of the experimental set up. A comparison of experimental data with the predicted results is not appropriate until repeatability is obtained with the test procedure. In retrospect, the precision required to obtain and hold in-plane strains of approximately one-tenth milli-inch and changes in length of the specimen on the order of one milli-inch may be unattainable with the Reihle 300,000 pound test machine.

B. COMPOSITE SPECIMENS

The ultimate shear force and ultimate moment were obtained for each composite plate in the same manner as in Ref. 4. Table II lists the results of the ultimate failure tests. No pull-through tests were conducted due to the difficulty with the testing procedure.

A hot acid resin digest test was performed on specimens from each composite plate fabricated in the composite lab. Fiber volume was used as a representative measure of fabrication quality and a relative measure of specimen strength, with 60 percent fiber volume the desired value. Using the procedure described in Ref. 11, actual fiber volumes were determined with a mean of 57.4 percent and a standard deviation of 4.0 percent. Discussion with Hercules Incorporated, the pre-preg manufacturer, indicated that this value was low and that their process achieves a 60 ±2 percent fiber volume.

The process of composite lay-up was an exacting and time-consuming exercise. Although the experience was invaluable, a more efficient approach would be the procurement of prepared laminate specimens in the desired size and fiber orientation.

The Wabash press used in the composite cure cycle was found to be difficult to adjust for pressure control. Its operation should be evaluated to ensure that the revised cure cycle accomplishes the same results as the recommended autoclave procedure.

VI. CONCLUSIONS

The experimental apparatus using the modified Reihle Testing Machine to develop an M-P-N generalized force field on an idealized wing skin test specimen has not met expectations. Efforts to achieve repeatable results were unsuccessful. Further investigation is necessary to develop confidence in the method of axial force application.

Predictions using the long thin plate theory were in general agreement with experimental data for small aspect ratios, i.e. equal to one or less. For lengths greater than four, test data showed that the theory did not agree well with experimental data.

The triaxial stress state at the fastener hole is complex and does not lend itself to a simple method of analysis.

The process for fabrication of composite plates in the Aeronautics Department Composite Lab results in composite plates with a significant range of strengths.

VII. RECOMMENDATIONS

Alternate methods of applying triaxial stresses to wing skin specimens should be pursued in order to develop a process which can represent this specialized loading condition.

Data recording while using the Reihle Testing Machine was inefficient, requiring a two-man operation. The testing machine should be instrumented to provide a continuous historical record using a strip chart or similar means.

The steady rate of application of the pull force would improve the experimental procedure. Although it may slightly alter the static loading condition, the smooth, slow load application rate would be much better for considerations of repeatability.

Consideration should be given to the procurement of composite specimens or plates when undertaking an experiment involving standard composite laminate specimens.

When laying up composite laminates an equal number of bleeder plies should be used on each side of the lay-up. The temperature gradient across dissimilar boundaries and non-uniform heat transfer characteristics may cause oil canning or warping of the finished plate. Close attention must be made to the lay-up sequence as the material properties of the laminate are a function of the lay-up sequence as well as the constituent properties. The result, again,

may be oil canning or warping of the plate. The cure cycle when initiated should not be interrupted. Restart is very difficult, if not impossible, to achieve. A 12 inch wide composite pre-preg tape is much more efficient for both cutting and lay up. A more consistent and uniform fiber orientation is also possible.

APPENDIX A

```
10 REM
20 REM   PROG CALCULATES 'PER UNIT LENGTH'
30 REM   VALUES. IF FORCES IN LBS(T1,P1)
40 REM   ARE USED VALUES MUST BE DIVIDED
50 REM   BY B AND ENTERED AS T & P.
60 REM
70 T=1250
80 H=0.09
90 L=4
100 E=10.3*(10↑6)
110 V=0.33
120 PRINT
130 PRINT "T="T;"H="H;"L="L
140 PRINT
150 FORMAT 6X,"P",6X,"S+T",7X,"S1",7X,"W",9X,"U"
160 WRITE (15,150)
170 INPUT P
180 I=0
190 INPUT N1,N2,N3
200 FOR U=N1 TO N2 STEP N3
210 D=(E*(H↑3))/(12*(1-(V↑2)))
220 DEF FNA(U)=(EXP(U)-EXP(-U))/2
230 DEF FNB(U)=(EXP(U/2)-EXP(-U/2))/2
240 DEF FNC(U)=(EXP(U)+EXP(-U))/2
250 DEF FND(U)=(EXP(U/2)+EXP(-U/2))/2
260 X1=FNA(U)
270 X2=FNB(U)
280 X3=FNC(U)
290 X4=FND(U)
300 Y1=1/(128*(U↑6))-(X2/(32*(U↑7)*X4))
310 Y2=(X1+U)/(128*(U↑7)*(X3+1))
320 Y3=(T*(H↑2)*D)/((U↑2)*(L↑4)*(P↑2)*12)
330 Y4=(D↑2)*(H↑2)/((P↑2)*(L↑6)*3)
340 Y=Y1+Y2+Y3-Y4
350 IF Y<0 THEN 390
360 Z=U
370 Z1=Y
380 NEXT U
390 I=I+1
400 IF I=4 THEN 460
410 N1=Z
420 N2=U
430 N3=(N2-N1)/20
440 GOTO 200
450 STOP
460 W1=(P*(L↑3)/(16*(U↑2)*D))*(1-(2*(X2/X4)/U))
470 S=((4*(U↑2)*D)/(L↑2))-T
480 M1=(P*L*X2)/(4*U*X4)
490 S1=(6*M1)/(H↑2)+(S+T)/H
500 FORMAT 2F8.0,2X,F8.0,F10.5,F10.6
510 WRITE (15,500)P;S+T;S1;W1;U
520 REM   VALUES PRESENTED IN 'PER UNIT LENGTH'
530 GOTO 170
540 END
```

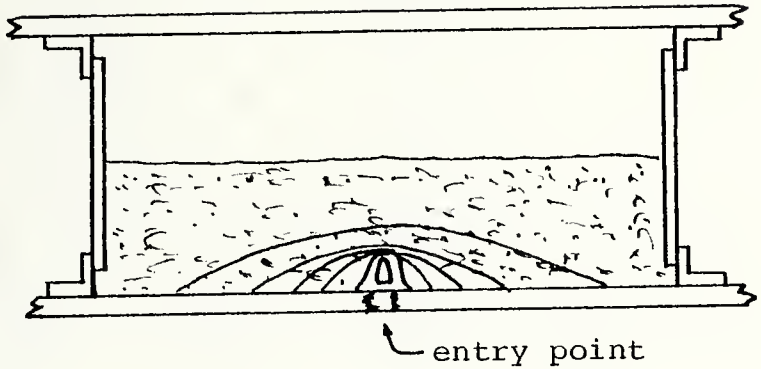

(a) Initial Impact

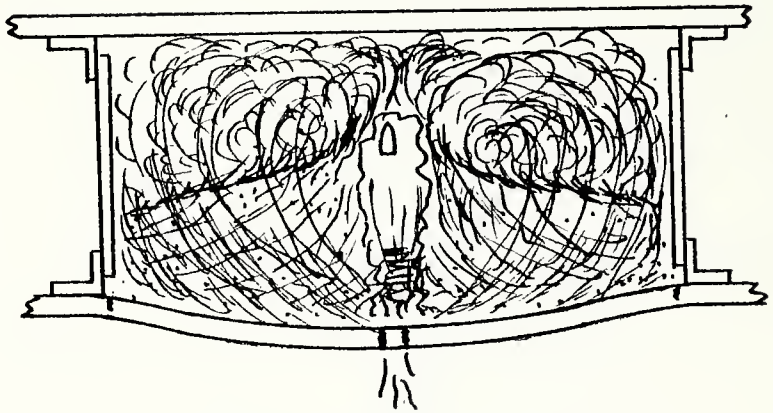

(b) Just Before Failure

FIGURE 1. DEVELOPMENT OF HYDRAULIC RAM IN TEST CELL

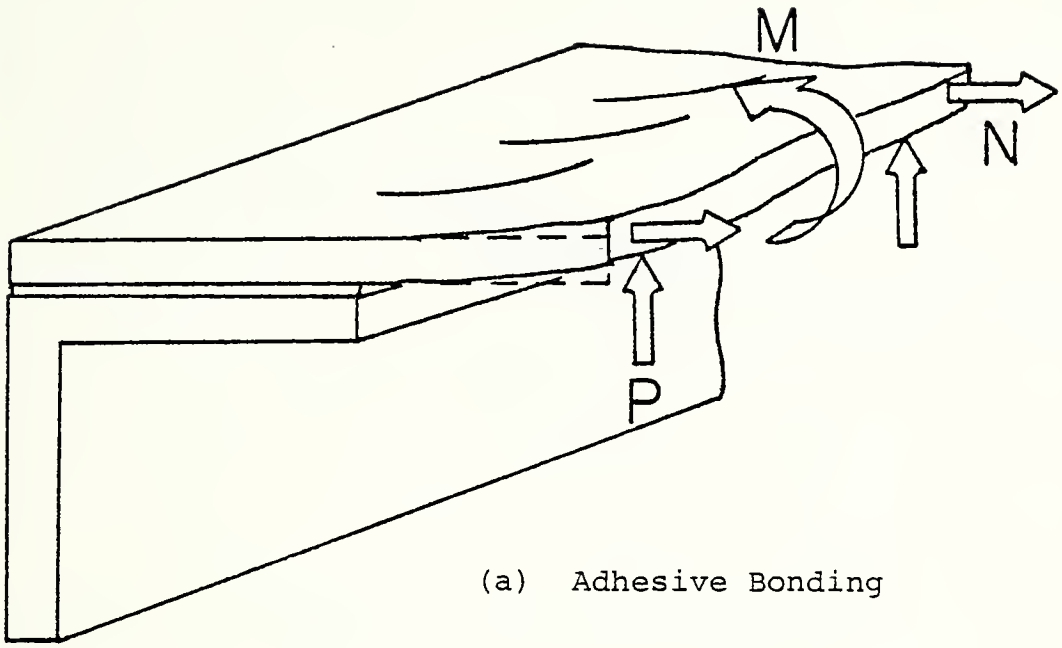

(a) Adhesive Bonding

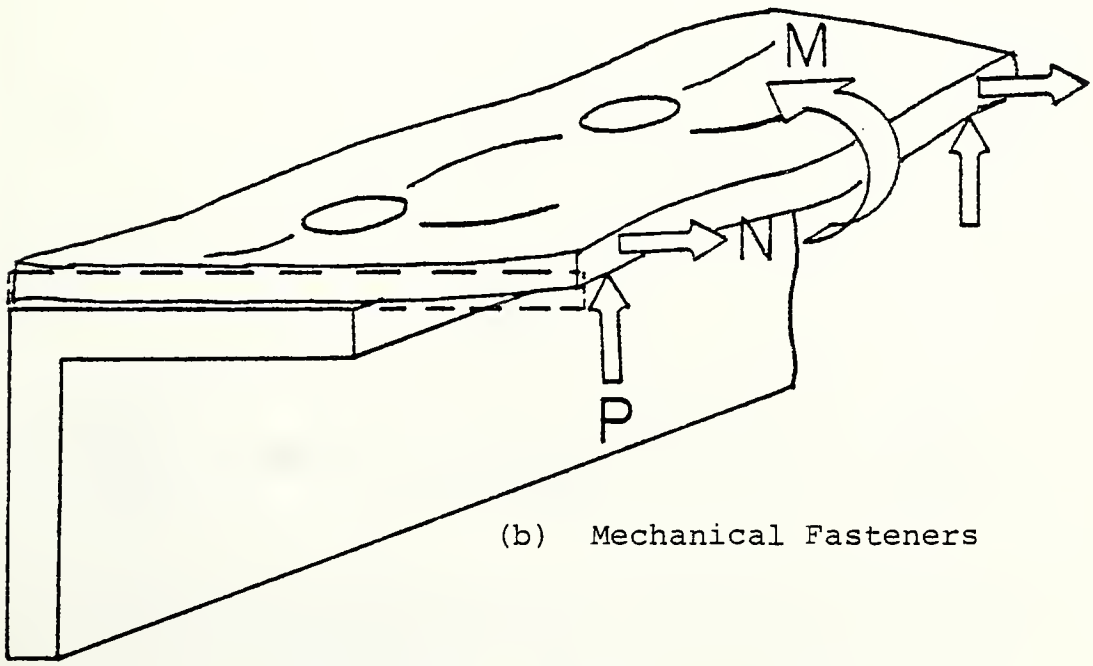

(b) Mechanical Fasteners

FIGURE 2. METHODS OF ATTACHMENT

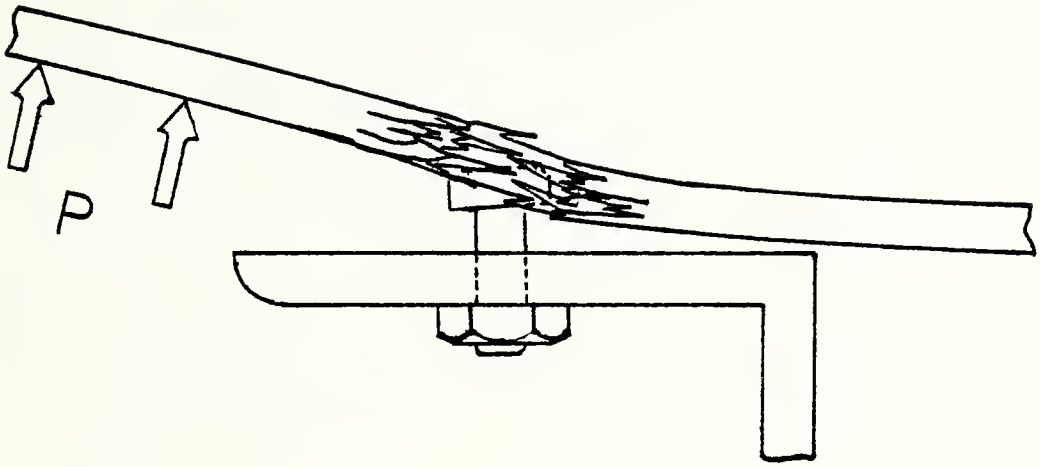

FIGURE 3. FASTENER PULL-THROUGH

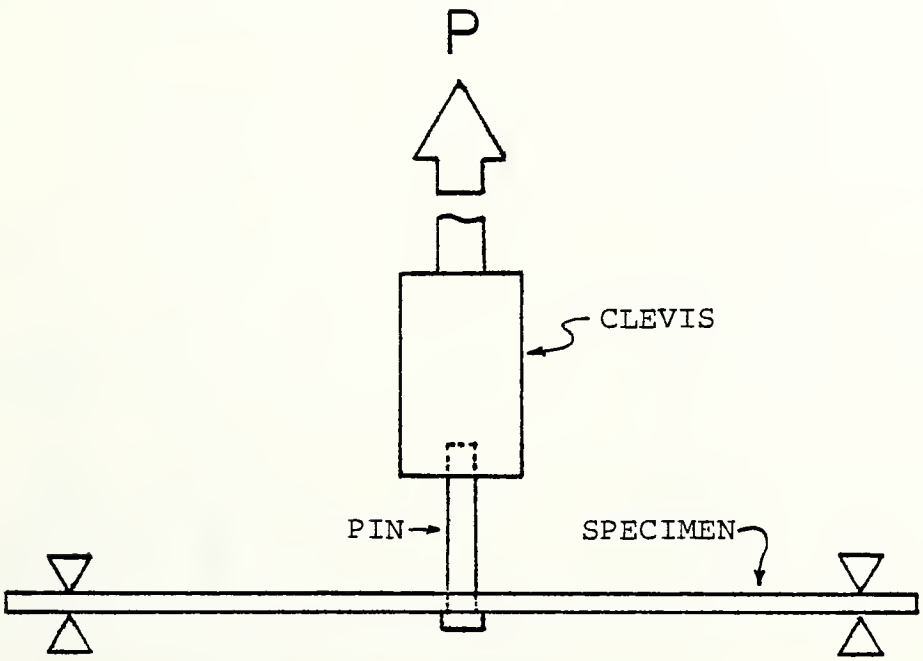

FIGURE 4. SIMPLY SUPPORTED FASTENER PULL-THROUGH SET UP

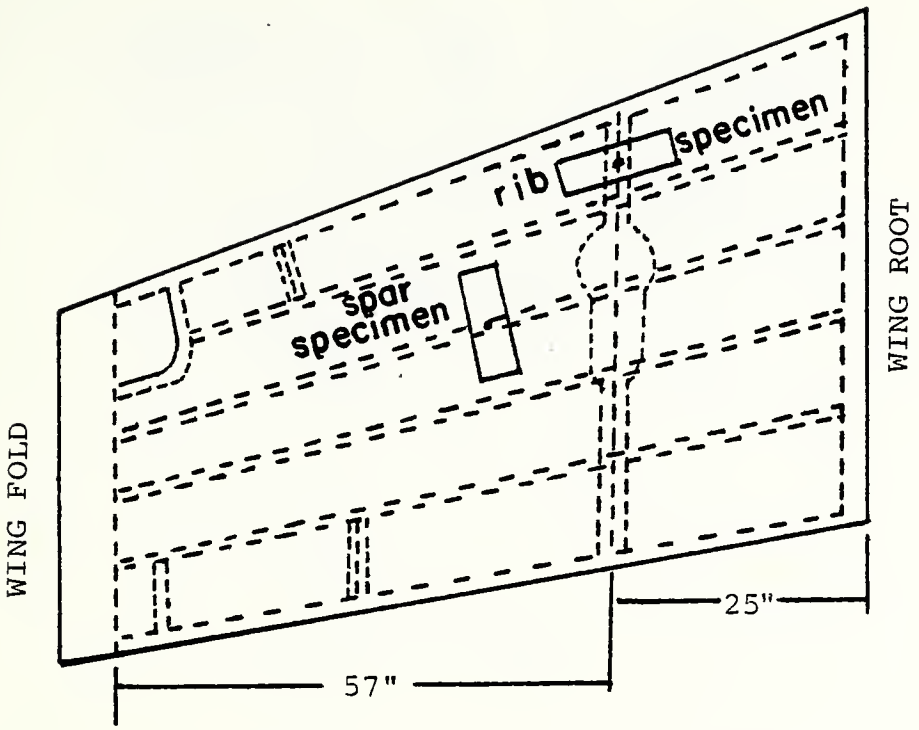

FIGURE 5. SPECIMEN ORIENTATION ON F-18 INBOARD WING STRUCTURE

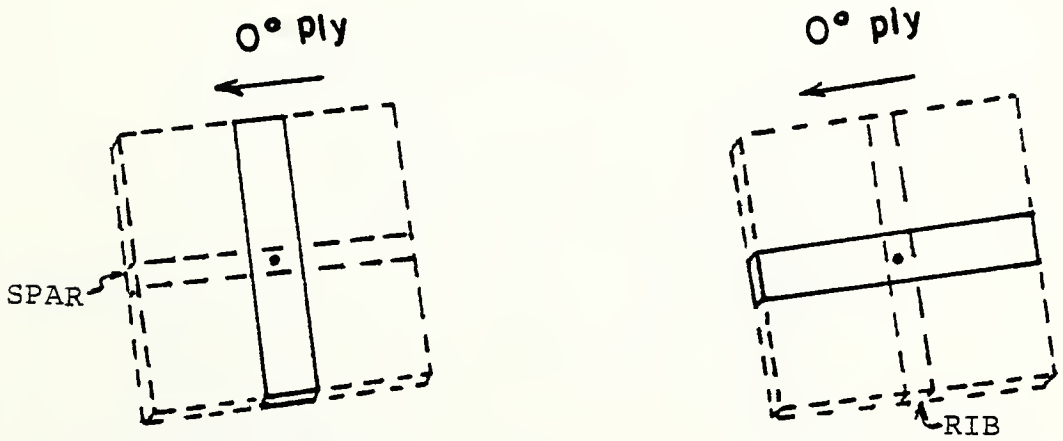

(a) Spar Specimen (b) Rib Specimen

FIGURE 6. SPECIMEN MODELS

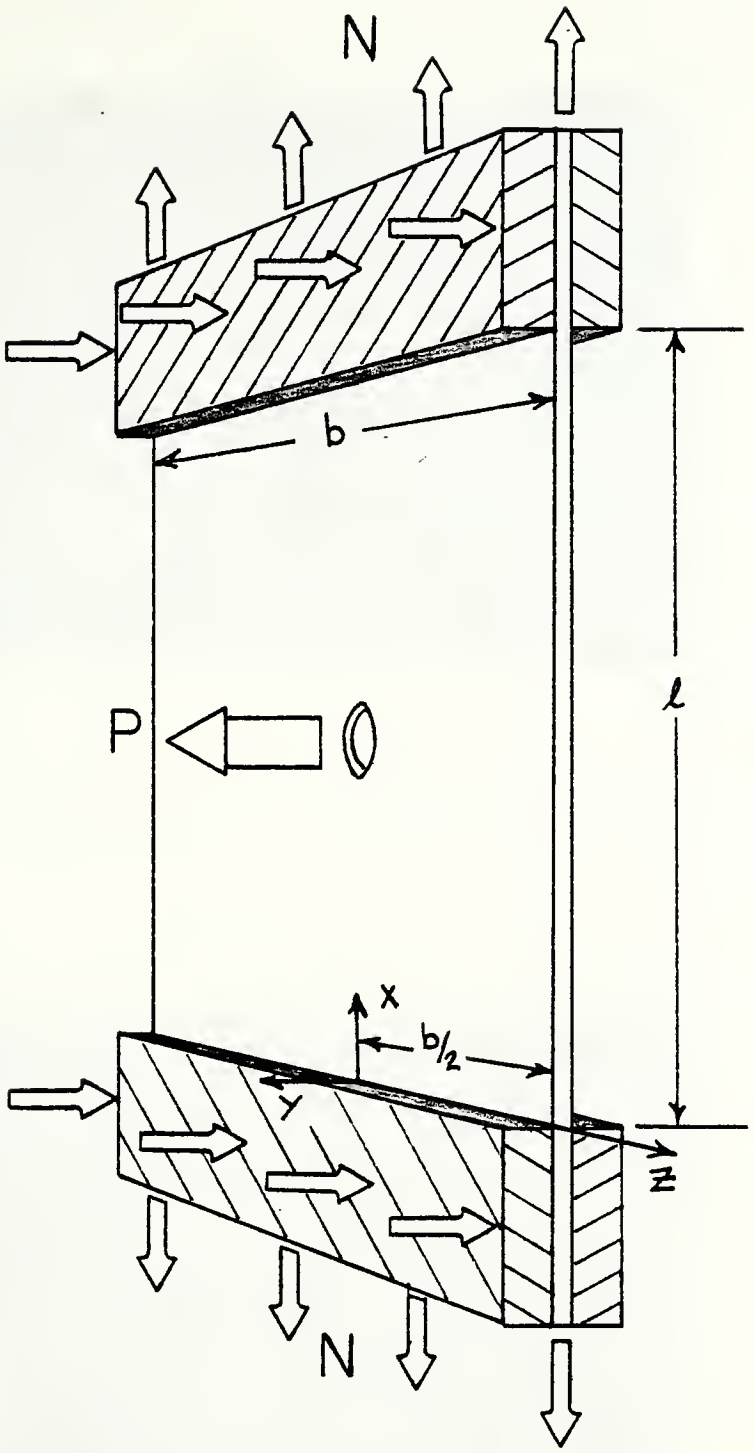

FIGURE 7. COMPOSITE LAMINATE TEST SPECIMEN

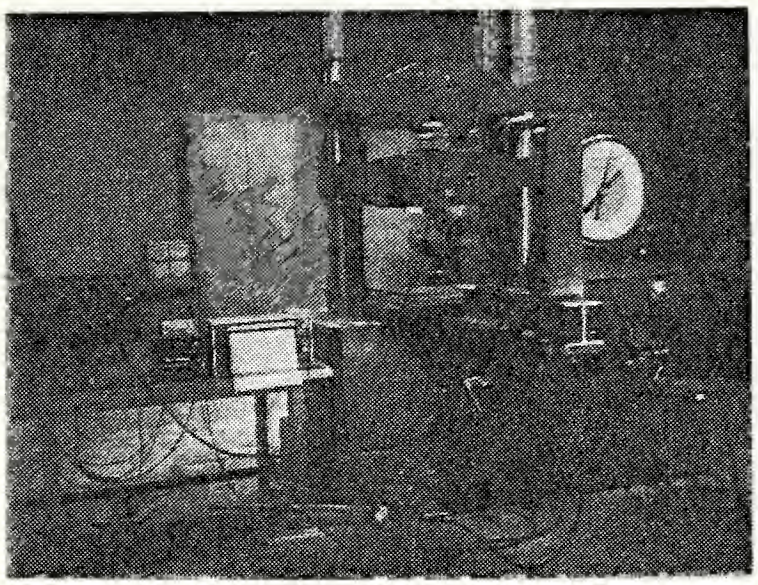

FIGURE 8. FASTENER PULL-THROUGH TEST SET UP

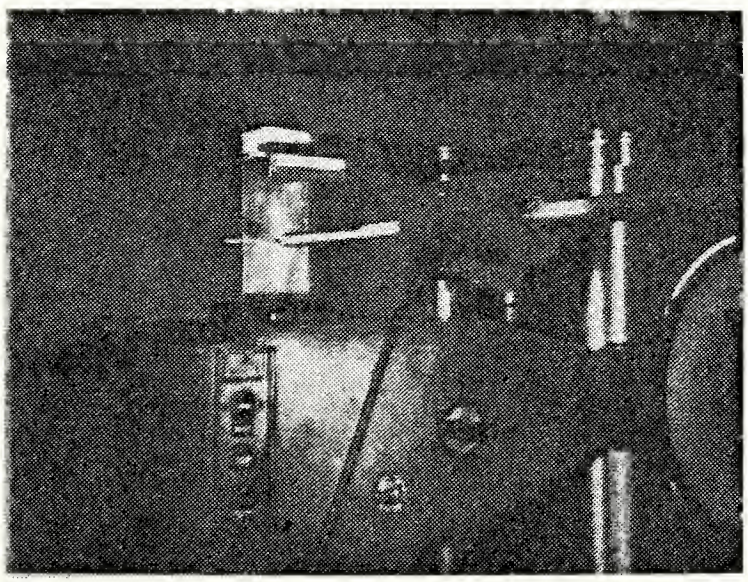

FIGURE 9. UNIFORM BENDING MOMENT TEST SET UP

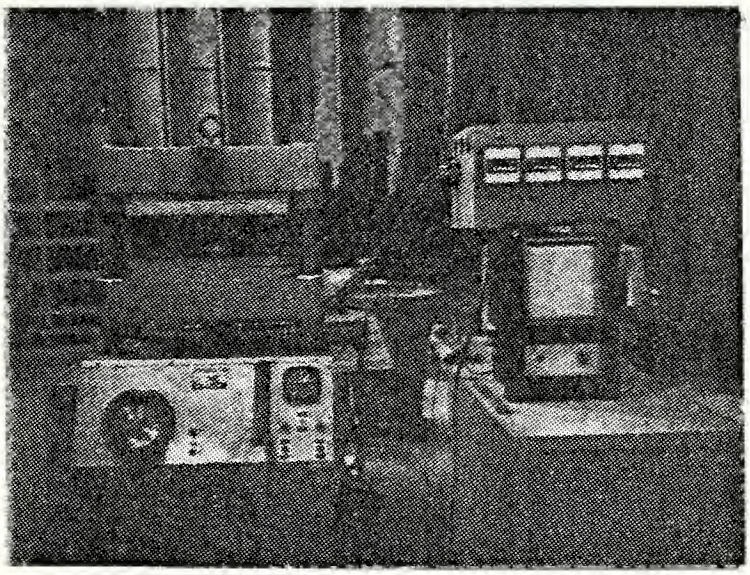

FIGURE 10. COMPOSITE CURE EQUIPMENT

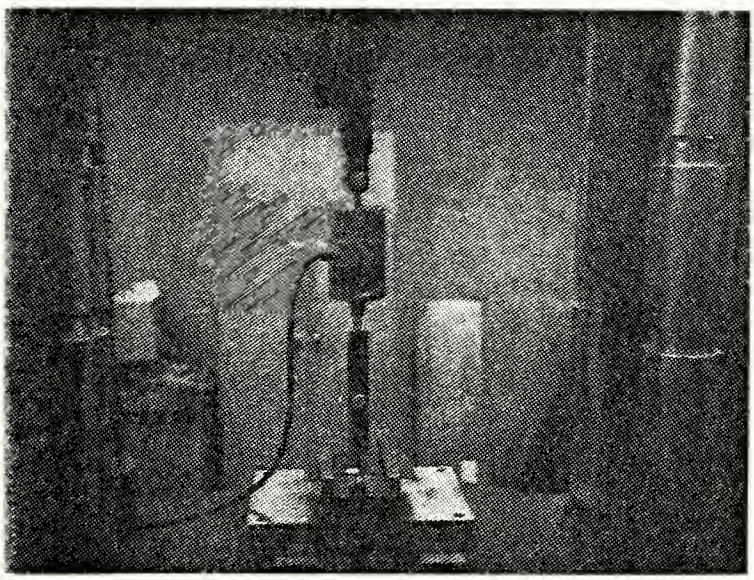

FIGURE 11. ULTIMATE BENDING MOMENT TEST RIG

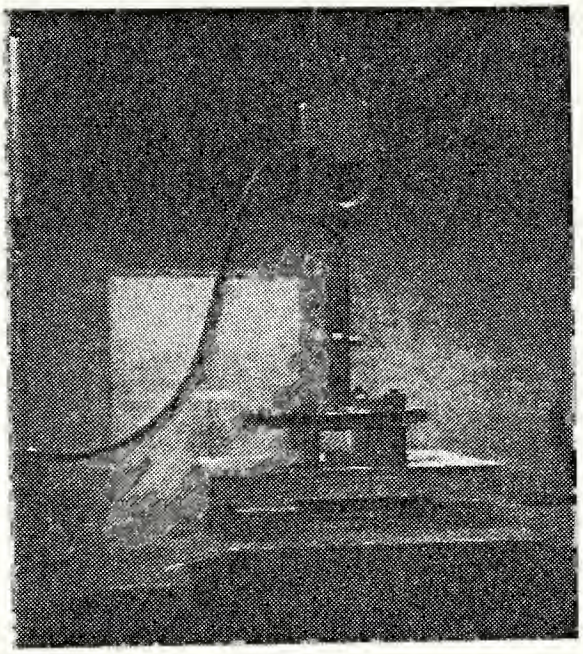

FIGURE 12. ULTIMATE SHEAR TEST RIG

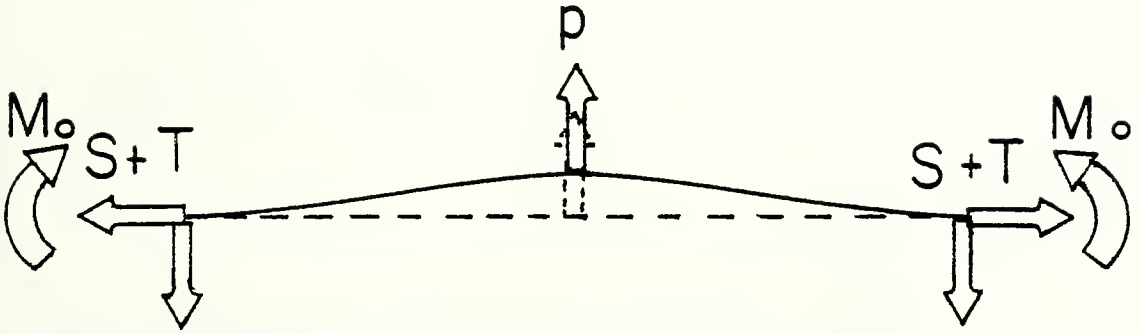

FIGURE 13. IDEALIZED WING SKIN LOADING DIAGRAM

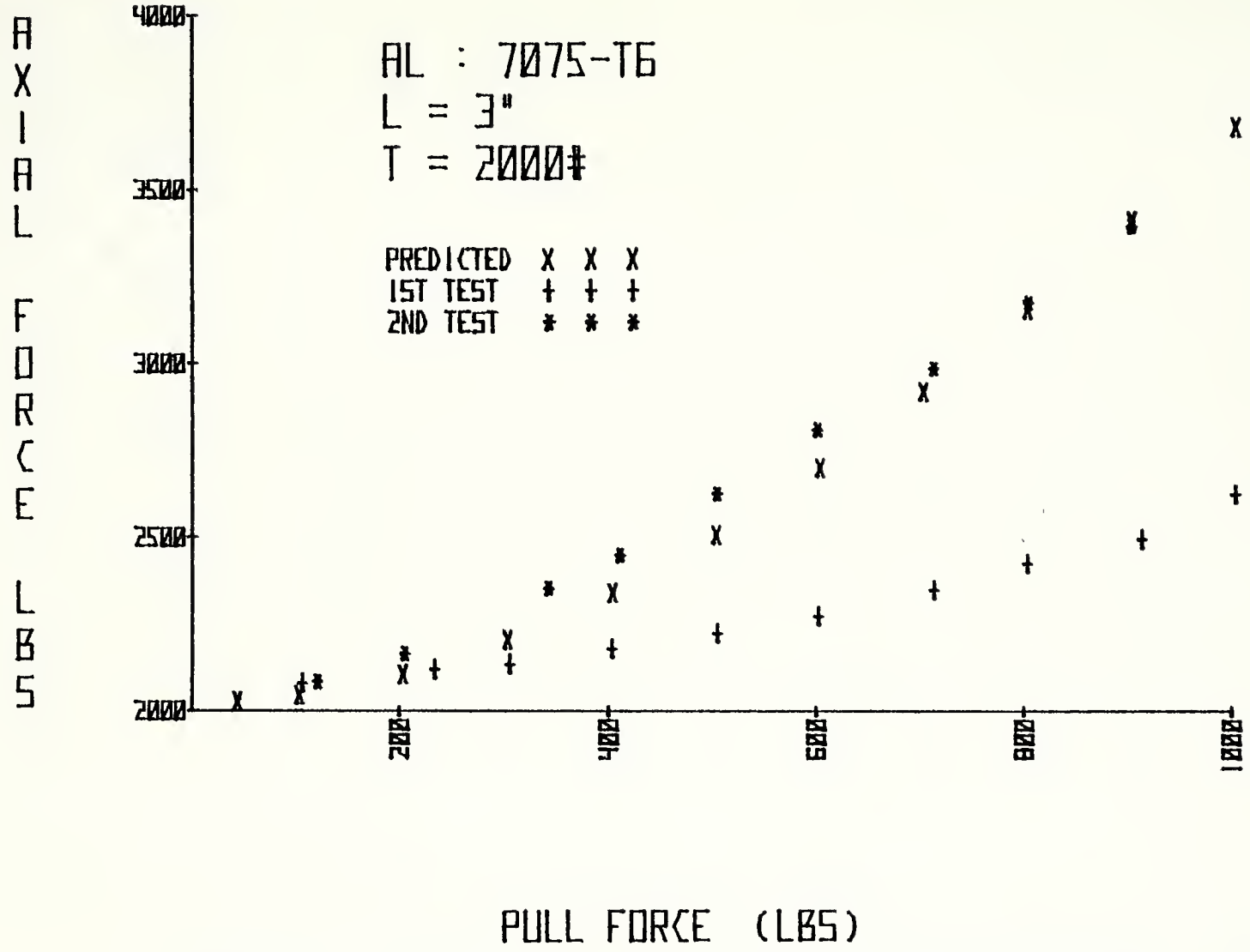

FIGURE 14a. COMPARISON OF EXPERIMENTAL RESULTS WITH PREDICTED FOR ALUMINUM SPECIMENS

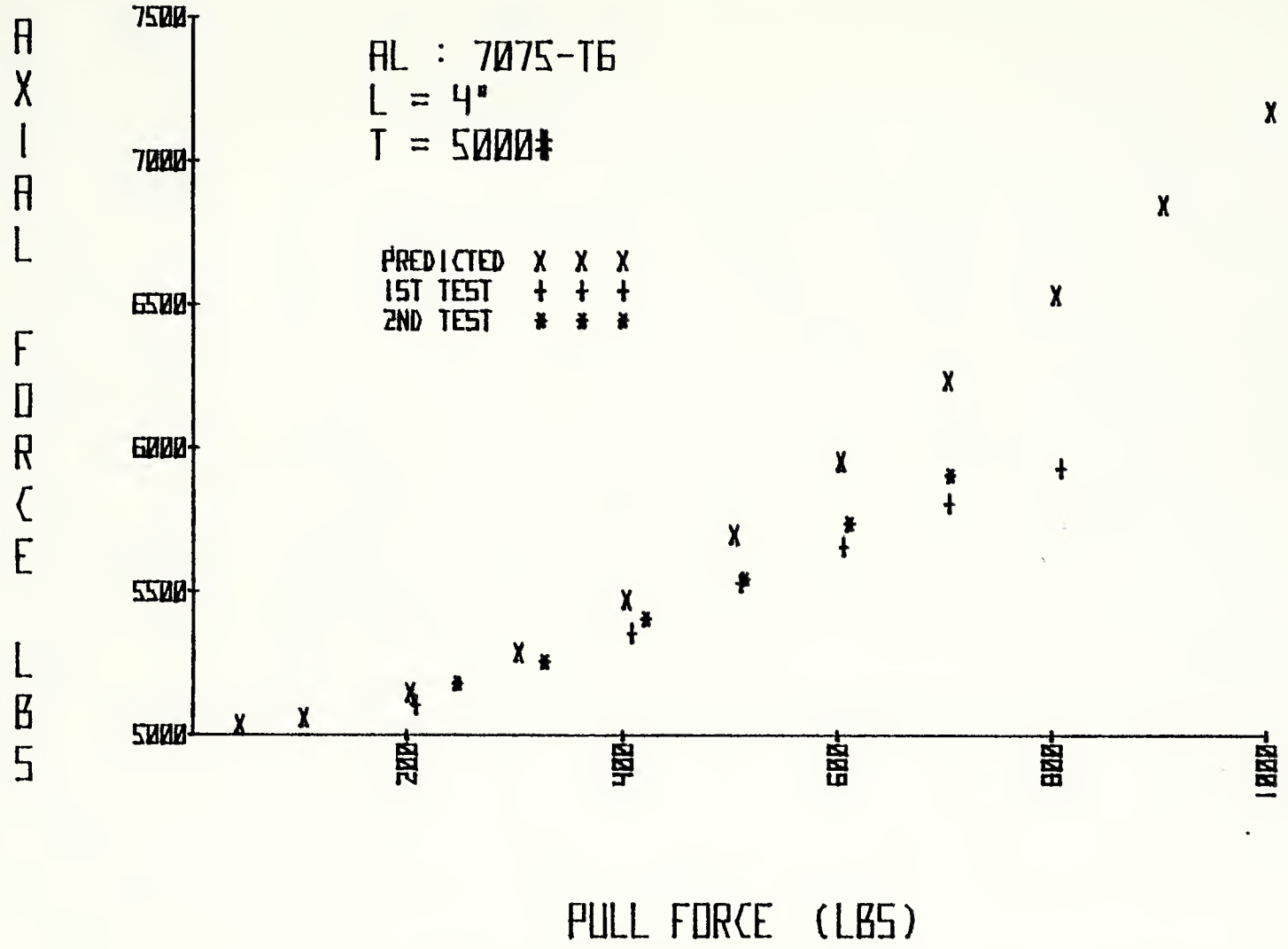

FIGURE 14b. COMPARISON OF EXPERIMENTAL RESULTS WITH PREDICTED FOR ALUMINUM SPECIMENS

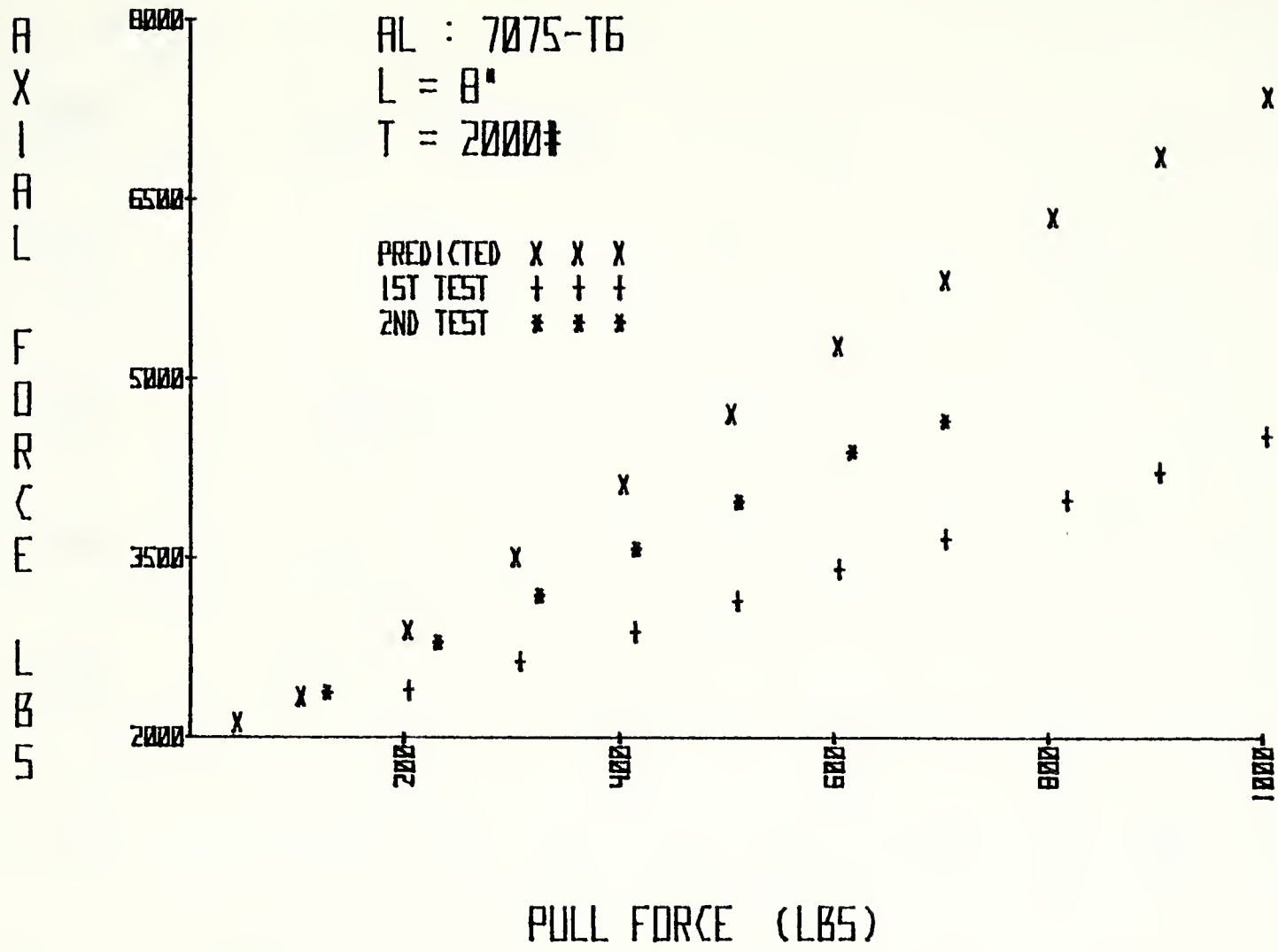

FIGURE 14c. COMPARISON OF EXPERIMENTAL RESULTS WITH PREDICTED FOR ALUMINUM SPECIMENS

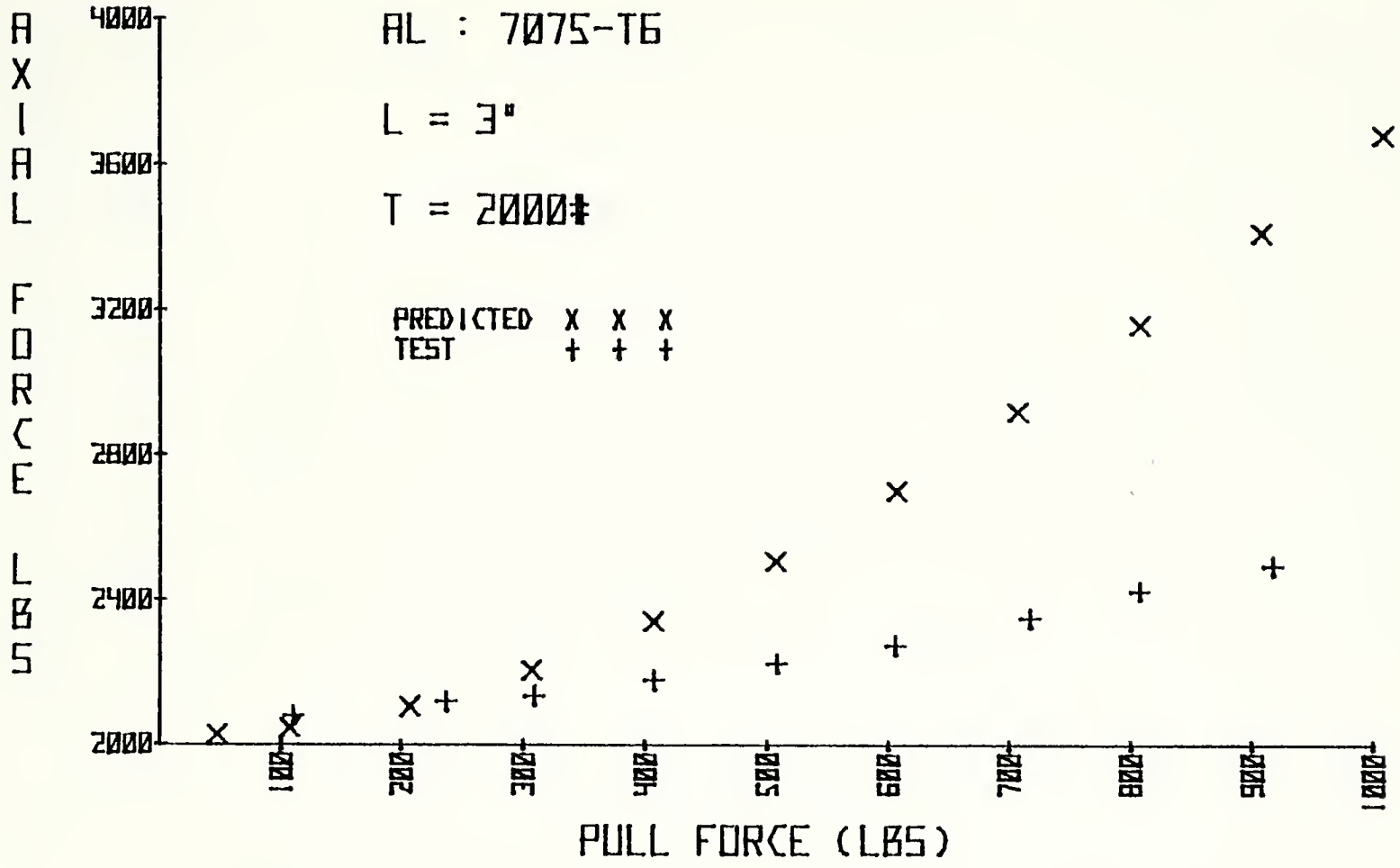

FIGURE 14d. COMPARISON OF EXPERIMENTAL RESULTS WITH PREDICTED FOR ALUMINUM SPECIMENS

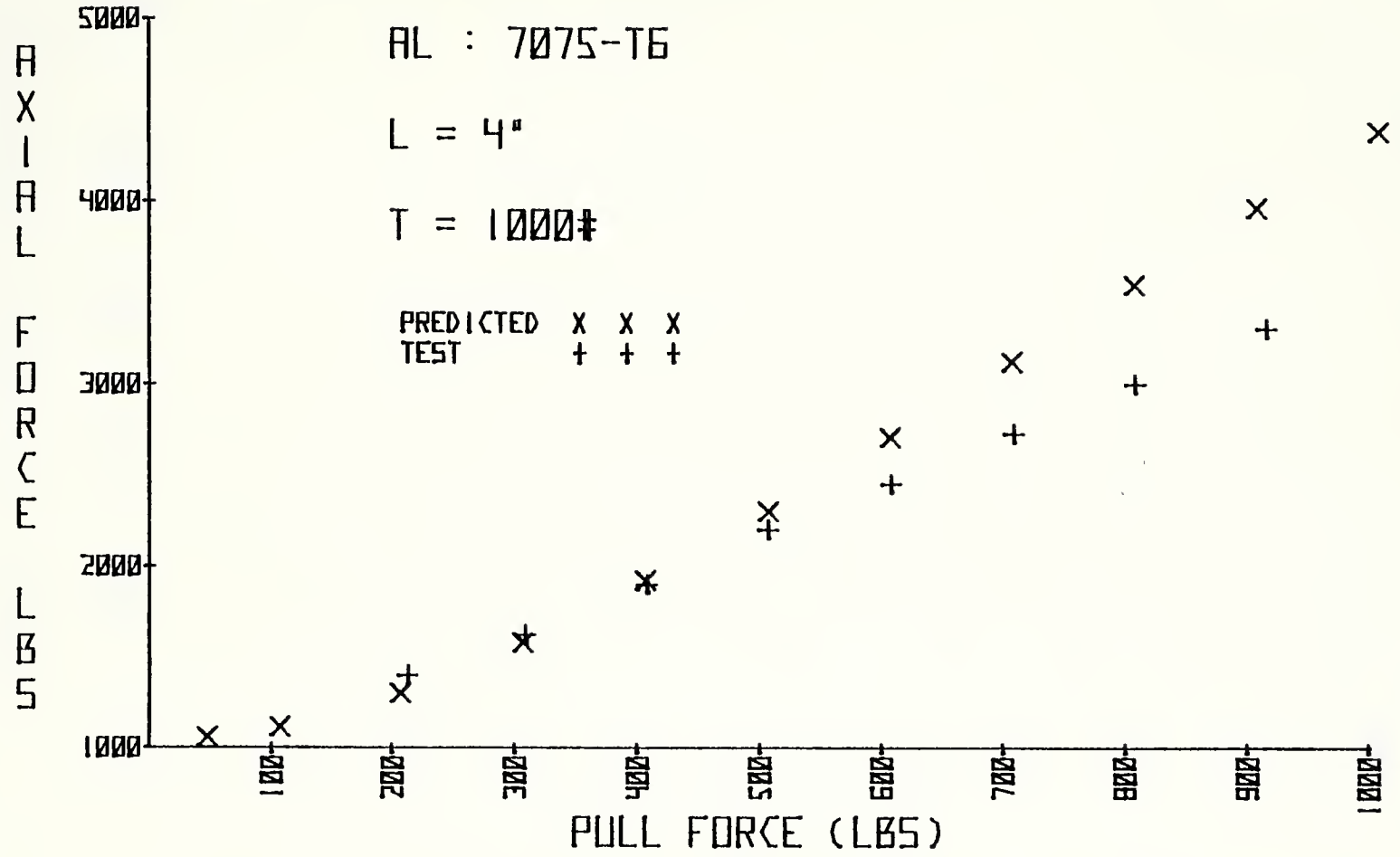

FIGURE 14e. COMPARISON OF EXPERIMENTAL RESULTS WITH PREDICTED FOR ALUMINUM SPECIMENS

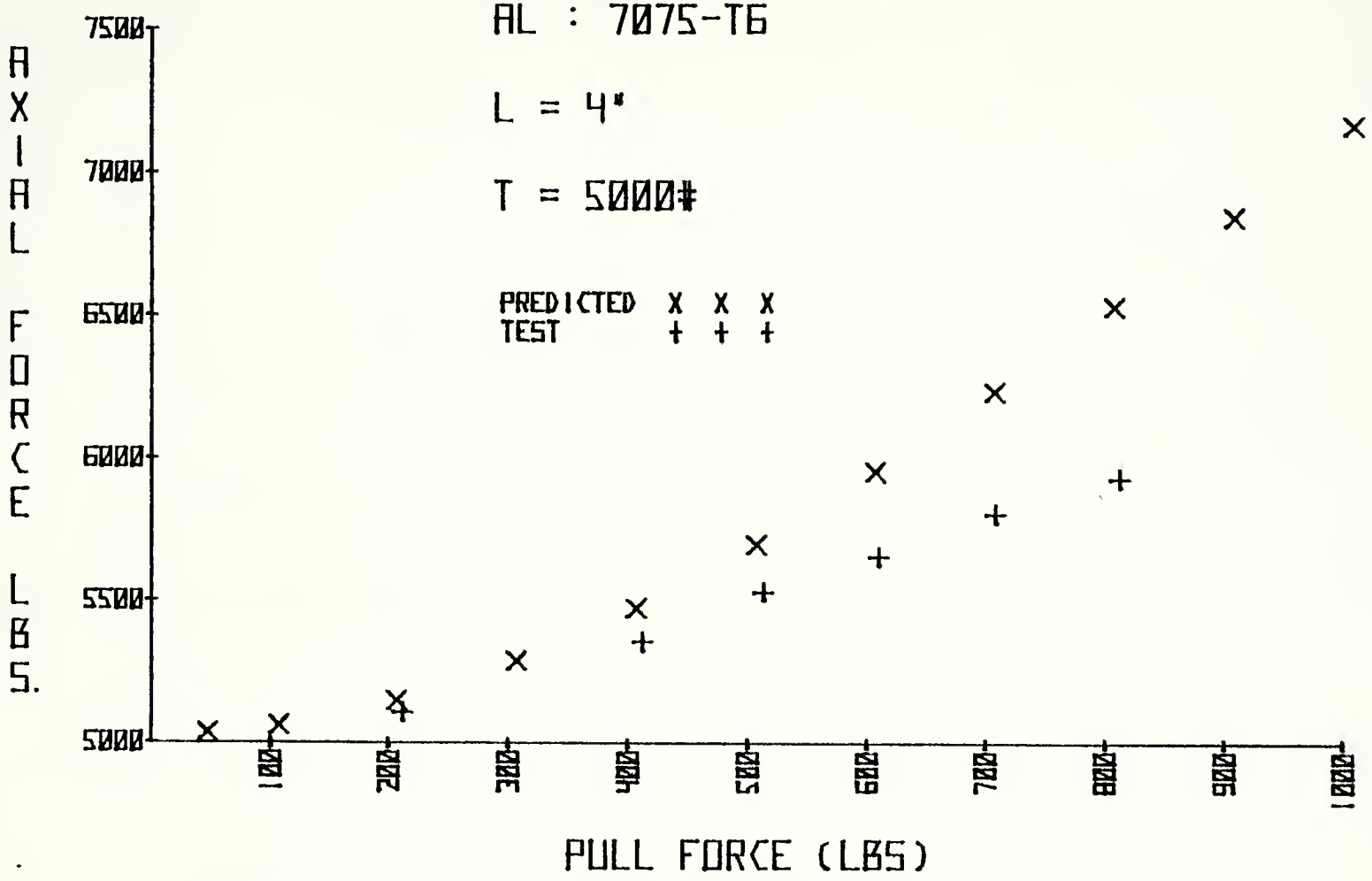

FIGURE 14f. COMPARISON OF EXPERIMENTAL RESULTS WITH PREDICTED FOR ALUMINUM SPECIMENS

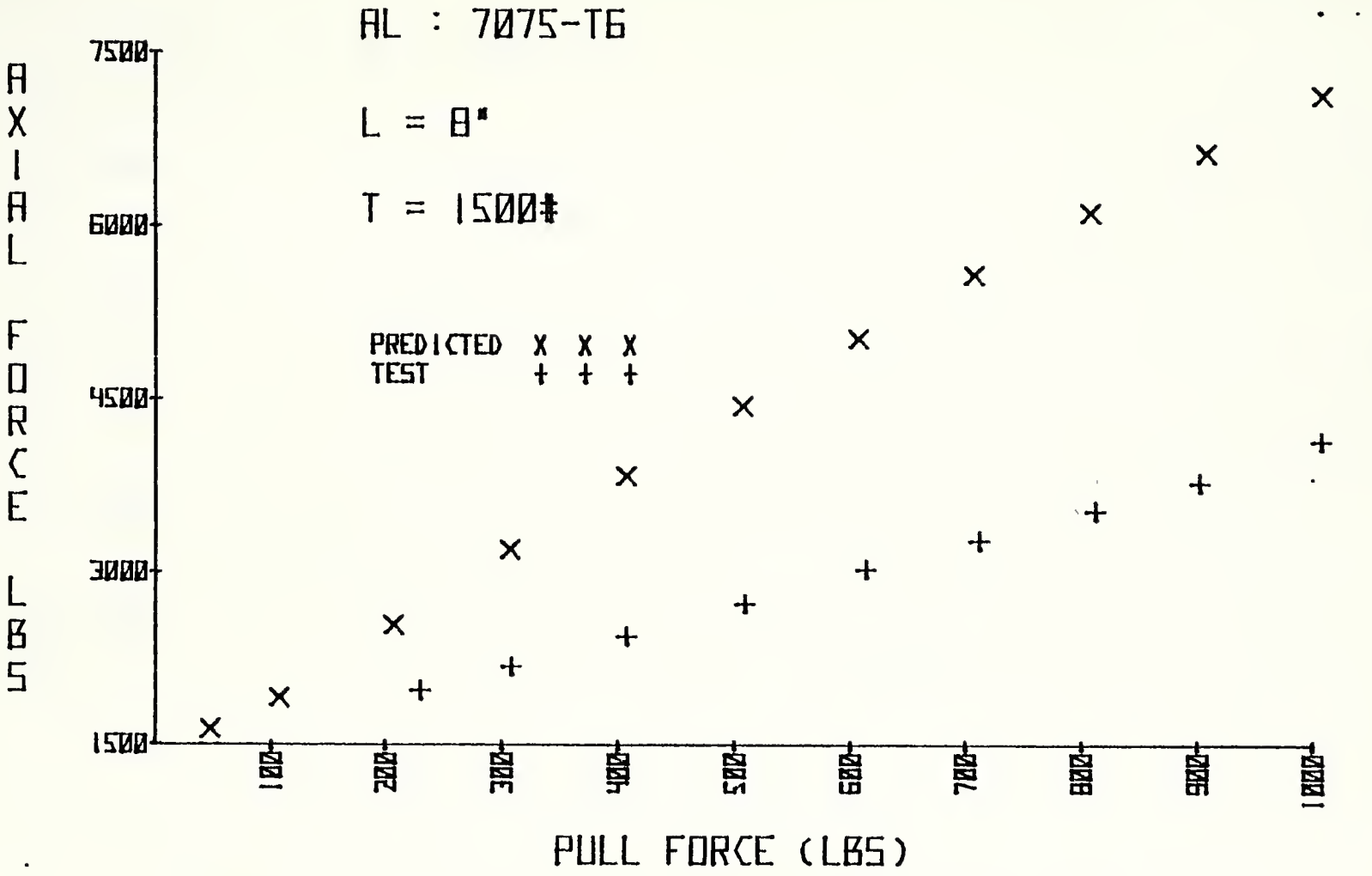

FIGURE 14g. COMPARISON OF EXPERIMENTAL RESULTS WITH PREDICTED FOR ALUMINUM SPECIMENS

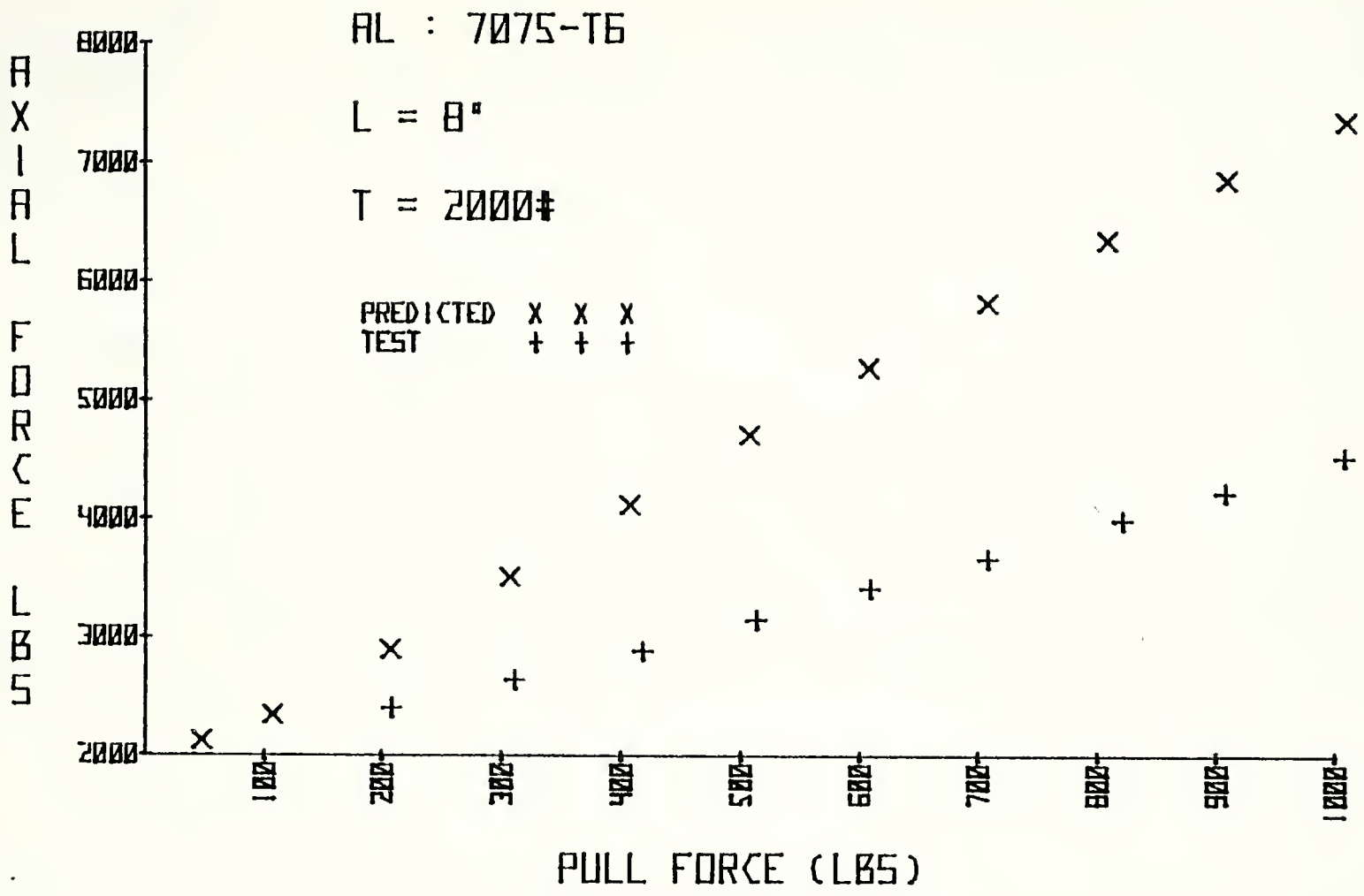

FIGURE 14h. COMPARISON OF EXPERIMENTAL RESULTS WITH PREDICTED FOR ALUMINUM SPECIMENS

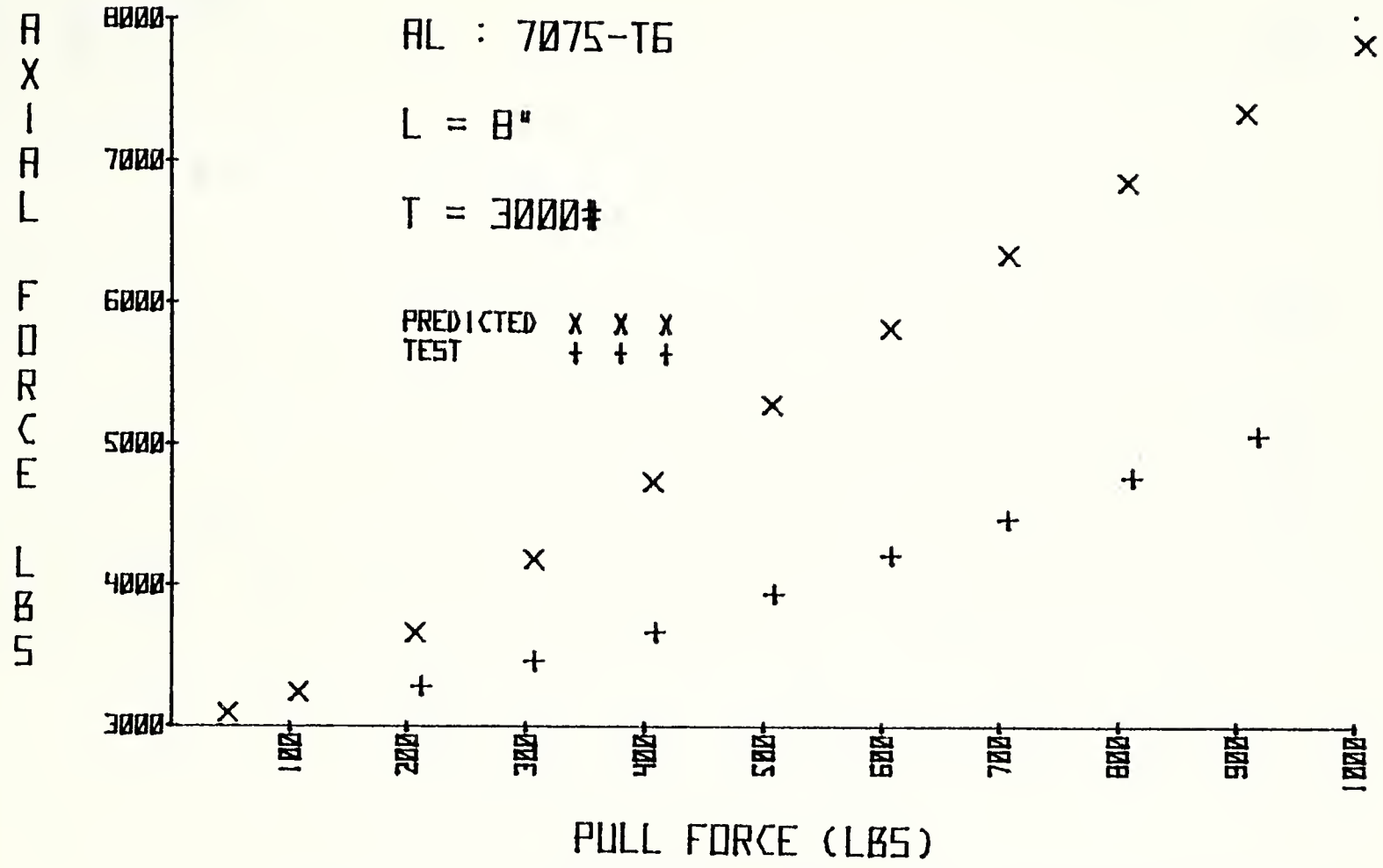

FIGURE 14i. COMPARISON OF EXPERIMENTAL RESULTS WITH PREDICTED FOR ALUMINUM SPECIMENS

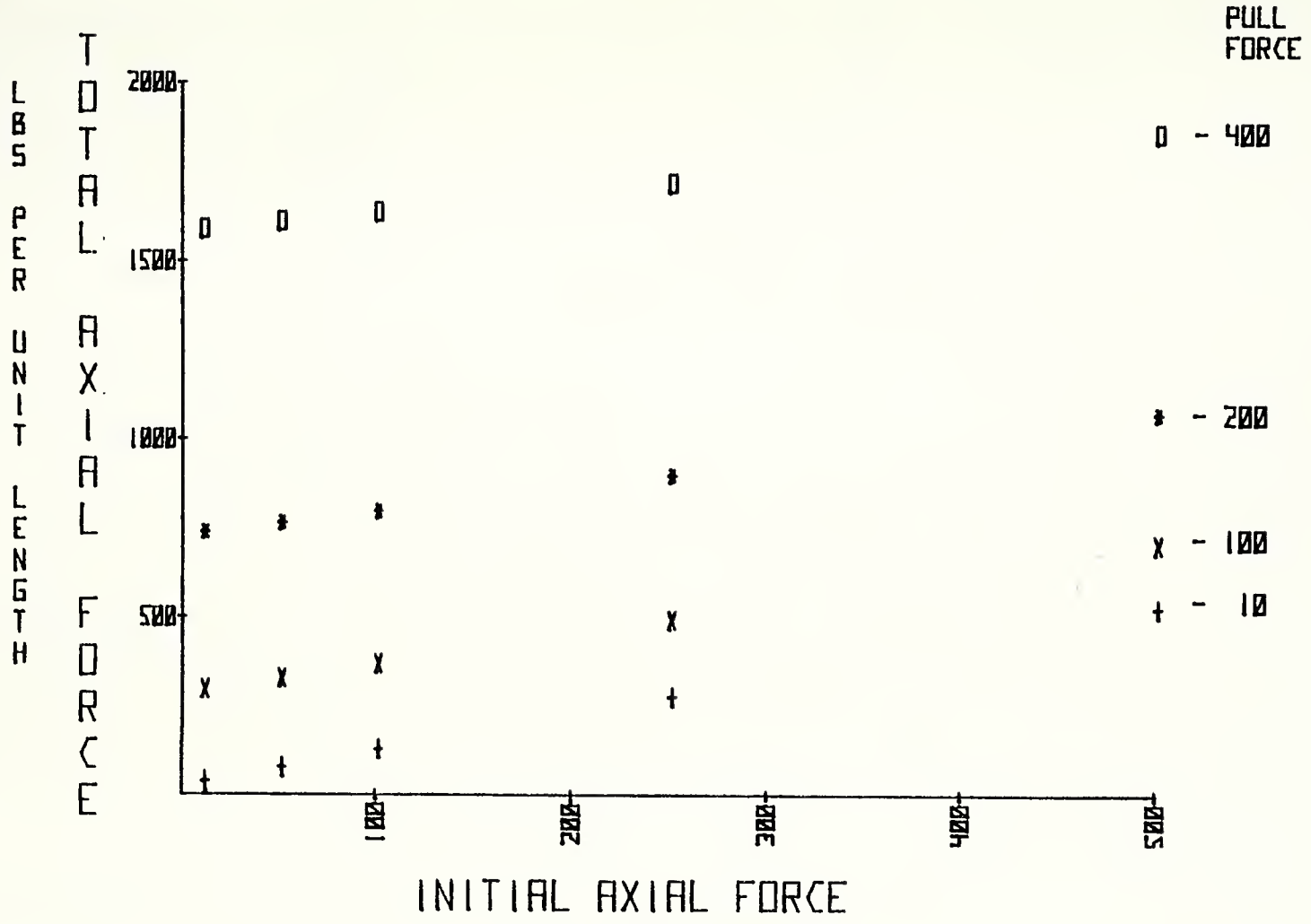

FIGURE 15. PLOT OF INITIAL TENSILE LOAD VERSUS TOTAL AXIAL FORCE FOR CONSTANT PULL FORCE

TABLE I. ULTIMATE FAILURE TEST RESULTS

(a) Ultimate Shear Test, ℓ = 4"

Plate #	Specimen #	P_{ult} at Failure (lbs)
1	51	1110
2	61	1450
3	71	950
4	81	1100
5	91	908

(b) Ultimate Tensile Test

Plate #	Specimen #	P_{ult} at Failure (lbs)
1	52	23500
2	62	17000
3	72	14600
4	82	14200
5	92	16450

(c) Ultimate Bending Test

Plate #	Specimen #	P_{ult} (lbs)	M_{ult} (lb-in)
1	53	670	670
2	63	895	895
3	73	360	360
4	83	763	763
5	93	703	703

TABLE II. COMPOSITE SPECIMEN ORIENTATION

Orientation	Specimen Number	Specimen Length (in)
Spar:	66	6
	74	4
	75	2
	76	4
	77	2
Rib:	55	4
	56	5
	57	4
	64	6
	65	6
	84	4
	85	1 1/4
	86	2
	87	2
	94	4
	95	1 1/4
	96	2
	97	1 1/4

TABLE III. MATERIAL PROPERTIES

Aluminum 7075-T6

F_{tu} = 79 KSI

F_{ty} = 70 KSI

F_{su} = 47 KSI

F_{cy} = 71 (longitudinal)

74 (transverse)

$E = 10.3 \times 10^6$ PSI

$= .33$

Graphite Epoxy $[0/\pm45/90]_s$

$E_{11} = 21 \times 10^6$ KSI

$E_{22} = 1.7 \times 10^6$ KSI

$G_{12} = .65 \times 10^6$ KSI

$\nu_{12} = .21$

$\nu_{12} = .017$

LIST OF REFERENCES

1. Duva, A.N., Hydraulic Ram Effect on Composite Fuel Cell Entry Walls, M.S.A.E. Thesis, Naval Postgraduate School, Monterey, CA., March 1976.

2. Ball, R.E., "Structural Response of Fluid-Containing Tanks to Penetrating Projectiles (Hydraulic Ram) — A Comparison of Experimental and Analytical Results," Naval Postgraduate School, Report NPS-57Bp 76051, May, 1976.

3. Ezzard, H.S., Jr., A Study of the Failure of Joints in Composite Material Fuel Cells Due to Hydraulic Ram Loading, M.S.A.E. Thesis, Naval Postgraduate School, Monterey, CA., June 1976.

4. Freedman, R.N., A Study of Pull-Through Failures of Mechanical Fastened Joints, M.S.A.E. Thesis; Naval Postgraduate School, Monterey, CA., Sept. 1977.

5. Saba, D.L., Stress Concentration Around Holes in Laminated Fibrous Composites, M.S.A.E. Thesis and Report NPS-57Bt 75061, Naval Postgraduate School, Monterey, CA., June 1975.

6. Sprigg, R.G., An Experimental Study to Determine the Reduction in Ultimate Bending Moment of a Composite Plate Due to an Internal Delamination, M.S.A.E. Thesis, Naval Postgraduate School, Monterey, CA., Dec. 1977.

7. General Dynamics Convair Aerospace Division Report JTCG/AS-74-D-002, "Aircraft Nonnuclear Survivability/ Vulnerability Terms," June 1976.

8. Advanced Composites Design Guide, Third Edition, Vol. I, Design, Rockwell International Corporation, pgs. 1.0.2.1-8, Jan. 1973.

9. AGARD Report No. 660, Certification Procedures for Composite Structures, "U.S. Navy Certification of Composite Wings for the F-18 and Advanced Harrier Aircraft," by Weinberger, R.A.; Somoroff, A.R.; and Riley, B.L.; 44th Meeting of the Structures and Materials Panal of AGARD, April 1977.

10. Advanced Composites Design Guide, Third Edition, Vol. IV, Materials, Rockwell International Corporation, pgs. 4.2.4.1-16, Jan. 1973.

11. Linnander, R.J., Laboratory Development and Tensile Testing of Graphite/Glass/Epoxy Hybrid Composite Materials, M.S.A.E. Thesis, Naval Postgraduate School, Monterey, CA., June 1974.

12. Hercules Incorporated, Graphite Materials, April 1976.

13. Timoshenko, S. and Woinowsky-Krieger, S.; Theory Plates and Shells, 2nd ed., McGraw-Hill Book Company, 1959.

INITIAL DISTRIBUTION LIST

		No. Copies
1.	Defense Documentation Center Cameron Station Alexandria, Virginia 22314	2
2.	Library, Code 0142 Naval Postgraduate School Monterey, California 93940	2
3.	Department Chairman, Code 67 Department of Aeronautics Naval Postgraduate School Monterey, California 93940	1
4.	Assoc. Prof. R.E. Ball, Code 67Bp Department of Aeronautics Naval Postgraduate School Monterey, California 93940	1
5.	LCDR Wayne R. Hanley Naval Air Systems Command (AIR-530C) Washington, DC 20361	1

Thesis 181601
H1965 Hanley
c.1 The development and evaluation of an experimental apparatus for the investigation of fastener pull-through failure in graphite-epoxy laminates.